Traffic Flow Models Based on Queuing Theory for Analysis and Performance Evaluation

May 2022

A Research Report from the Pacific Southwest Region University Transportation Center

Ketan Savla, University of Southern California

Petros Ioannou, University of Southern California

Pacific Southwest Region UTC
University Transportation Center

USC Viterbi
School of Engineering

TECHNICAL REPORT DOCUMENTATION PAGE

1. Report No. PSR-19-17	**2. Government Accession No.** N/A	**3. Recipient's Catalog No.** N/A
4. Title and Subtitle Traffic Flow Models Based on Queuing Theory for Analysis and Performance Evaluation		**5. Report Date** May 2022 **6. Performing Organization Code** N/A
7. Author(s) Ketan Savla, ORCID ID: 0000-0002-1668-6380 Petros Ioannou, ORCID ID: 0000-0001-6981-0704		**8. Performing Organization Report No.** TBD
9. Performing Organization Name and Address METRANS Transportation Center University of Southern California University Park Campus, RGL 216 Los Angeles, CA 90089-0626		**10. Work Unit No.** N/A **11. Contract or Grant No.** USDOT Grant 69A3551747109
12. Sponsoring Agency Name and Address U.S. Department of Transportation Office of the Assistant Secretary for Research and Technology 1200 New Jersey Avenue, SE, Washington, DC 20590		**13. Type of Report and Period Covered** Final report (May 16, 2020 - July 31,2021) **14. Sponsoring Agency Code** USDOT OST-R
15. Supplementary Notes		

16. Abstract

A fundamental problem in traffic networks is driving under safety and limited physical space constraints. In this project, we study the interplay of these constraints with control and its impact on system level performance. This is done in the setting of a closed system, i.e., without arrival or departures, as well as in the setting with arrival and departures. In the first setting, we design longitudinal vehicle controllers and study the dynamics of a system of homogeneous vehicles on a single-lane ring road in order to understand the interplay of limited space, speed, and safety. Each vehicle in the system either operates in the cruise control mode or follows a vehicle ahead by keeping a safe time headway. We show that if the number of vehicles is less than a certain critical threshold, vehicles can occupy the limited space in many different configurations, i.e., different platoons of different sizes, and they converge to a uniform maximum speed while attenuating errors in the relative spacing upstream a platoon. If the number of vehicles exceeds the threshold, vehicles converge to a unique symmetric configuration and the equilibrium speed decreases as the number of vehicles increases. Next, we consider vehicle-to-vehicle (V2V) communication and show that it increases the critical number of vehicles that can travel with the maximum speed. We demonstrate the performance of the proposed controllers via simulation. In the second setting, we consider a generalization to allow entry of vehicles under a microscopic ramp metering control. Upon arrival, the vehicle dynamics is similar to the first setting. The vehicles leave the system from off-ramps upon completion of their respective trips. We consider ramp metering policies inspired by scheduling policies from spatial queues with reuse, and provide performance analysis in terms of throughput.

17. Key Words Queuing Theory, Traffic Flow Models, Closed System, Ramp Metering, Performance Analysis	**18. Distribution Statement** No restrictions.		
19. Security Classif. (of this report) Unclassified	**20. Security Classif. (of this page)** Unclassified	**21. No. of Pages** 26	**22. Price** N/A

Form DOT F 1700.7 (8-72) Reproduction of completed page authorized

Disclaimer Statement

The contents of this report reflect the views of the authors, who are responsible for the accuracy of the data and information presented herein. This document is disseminated under the sponsorship of the Department of Transportation, University Transportation Centers Program, the California Department of Transportation and the METRANS Transportation Center in the interest of information exchange. The U.S. Government, the California Department of Transportation, and the University of Southern California assume no liability for the contents or use thereof. The contents do not necessarily reflect the official views or policies of the State of California, USC, or the Department of Transportation. This report does not constitute a standard, specification, or regulation.

Abstract

A fundamental problem in traffic networks is driving under safety and limited physical space constraints. In this project, we study the interplay of these constraints with control and its impact on system level performance. This is done in the setting of a closed system, i.e., without arrival or departures, as well as in the setting with arrival and departures.

In the first setting, we design longitudinal vehicle controllers and study the dynamics of a system of homogeneous vehicles on a single-lane ring road in order to understand the interplay of limited space, speed, and safety. Each vehicle in the system either operates in the cruise control mode or follows a vehicle ahead by keeping a safe time headway. We show that if the number of vehicles is less than a certain critical threshold, vehicles can occupy the limited space in many different configurations, i.e., different platoons of different sizes, and they converge to a uniform maximum speed while attenuating errors in the relative spacing upstream a platoon. If the number of vehicles exceeds the threshold, vehicles converge to a unique symmetric configuration and the equilibrium speed decreases as the number of vehicles increases. Next, we consider vehicle-to-vehicle (V2V) communication and show that it increases the critical number of vehicles that can travel with the maximum speed. We demonstrate the performance of the proposed controllers via simulation.

In the second setting, we consider a generalization to allow entry of vehicles under a microscopic ramp metering control. Upon arrival, the vehicle dynamics is similar to the first setting. The vehicles leave the system from off-ramps upon completion of their respective trips. We consider ramp metering policies inspired by scheduling policies from spatial queues with reuse, and provide performance analysis in terms of throughput.

Contents

List of Figures

1 Disclosure

K. Savla has financial interest in Xtelligent, Inc.

2 Acknowledgements

This research was performed in collaboration with M. Pooladsanj at the University of Southern California.

3 Introduction

Traffic congestion has costed billions of dollars, hours, and gallons of fuel in the past years [1]. While this congestion is a direct consequence of high travel demand competing to utilize the limited supply of road networks in a safe manner [2, 3], it is magnified by poor human drivers' response to various disturbance [4]. It has been reported that Connected and Autonomous Vehicles (CAVs) have the potential to compensate for human errors and corresponding delays to effectively improve the throughput and capacity of highways [4]. Hence, it is important to understand the interplay of the limited supply of road networks, which we shall refer to as *bounded space*, and safety constraints in the microscopic traffic studies of CAVs.

The impact of CAVs on traffic flow in the longitudinal direction is often evaluated by considering autonomous vehicles on an unbounded single lane road with no passing. The majority of research in this direction consider a platoon of vehicles and assume that the leader of the platoon follows a desired speed trajectory. The objective is then to design state-feedback throttle/brake controllers for the following vehicles such that they can adjust their speed to the speed of the leader while keeping a safe distance from the next vehicle [5,6]. The dynamical analysis of the following vehicles provide results on collision avoidance, attenuation of errors upstream the platoon, the effect of delay in the system performance, ride comfort, and the impacts of integration of communication channels [5–15]. The aforementioned research efforts focus on evaluating the performance of CAVs when they are already in the vehicle following mode. In practice, the performance of CAVs in handling different situations such as switching between different modes of operation must be also taken into account. In [16], a supervisory controller was designed and analyzed which was responsible for interacting with the throttle/brake controller, choosing the proper mode of operation, e.g., cruise control or vehicle following, the transition between these modes, and detecting any irregular behavior such as an emergency stopping situation. In all of these studies, increasing the size of the platoon does not affect the speed or density since it is assumed that the platoon leader can follow the desired trajectory without being interrupted. Therefore, the trade-offs between bounded space, safety, and speed is studied by performing steady state capacity analysis [17] where the capacity is calculated by assuming that the vehicles are already at steady state.

It is of more practical interest to study these trade-offs when vehicles are not at steady state. While studying vehicles on a fixed-length section of the road with boundary conditions is a possibility, we choose a ring road set up because of the following advantages. First, it is analytically easier to study the dynamics of vehicles on a ring road compared to its straight line analogue. Second, the ring road can capture the high-density traffic dynamics in which every vehicle follows a vehicle in front [18–20]. Third, it gives the flexibility for a vehicle to switch between cruise control and vehicle following depending on the local traffic. Moreover, experimental evidence [21] suggests that the ring road setup can capture the formation of stop-and-go waves in the absence of bottlenecks/lane changes. Our results in this project indicate that the conditions for stability and attenuation of errors upstream of a platoon, as well as the conclusions about the dissipation of stop-and-go waves on a ring road are consistent with previous results on a straight line. Furthermore, the macroscopic quantities discussed in this project such as capacity, critical, and jam densities, are independent of the circumference of the ring road and are identical to their analogues obtained by previous steady-state capacity analysis. In spite of the scale invariance property of the ring road setup, the literal interpretation of the model for real highways is perhaps best done at large circumferences to avoid pathological scenarios induced by rigid space constraint at small circumferences.

Inspired in part by [21] and the theoretical advantages of a ring road model, there has been recent dynamical analysis on this setup for mixed-autonomy [18–20, 22–24]. The foci of the analytical

aspects of these works, however, is on the formation of traffic jams and their dissipation using autonomous vehicles for a high density scenario, without explicit consideration of safety. Earlier work from the authors [25] explicitly included the safety constraint for a simple vehicle model. However, the impact of V2V communication and coordination of vehicles on the bounded space was not addressed. Practical bounds on the acceleration of vehicles was not considered either.

In this project, we consider homogeneous automated vehicles on a single lane ring road. We adopt a nonlinear vehicle model with first-order engine dynamics from [26] derived from Newton's second law of motion. We design state-feedback control laws based on feedback linearization to control the throttle and brake commands. Two different settings are considered.

In the first setting, we consider a closed system, i.e., without external arrivals or departures of vehicles. Within this setting we consider two scenarios. In the first scenario, we assume that vehicles do not communicate and there is no coordination. Each vehicle either follows a constant speed trajectory, i.e., the cruise control mode, or safely follows the vehicle ahead, i.e., the vehicle following mode, by keeping a safe time headway. Transitioning between modes of operation is determined by a combination of relative spacing and speed signals and is handled by the vehicle's supervisory controller as discussed in [16]. It is analytically shown that the equilibrium of this dynamical system leads to the well-known triangular fundamental diagram. In other words, the interplay of bounded space, speed limit, and safety can be quantified in a straightforward manner with this problem formulation. We explicitly characterize the critical density ρ_c of the fundamental diagram, at which the flow is maximized, in terms of system parameters (time headway constant, free flow speed, minimum standstill safety distance, and length of each vehicle). In the second scenario, we assume that vehicles are also able to communicate their braking capabilities and their instantaneous acceleration with their following vehicle. We show that V2V communication increases ρ_c and the capacity of the road compared to the first scenario, thus it enhances the free flow region of the fundamental diagram. We demonstrate the performance of the controllers by simulating different scenarios.

In the second setting, we model arrivals and departures of vehicles. Vehicles arrival to the on-ramps and the destination off-ramp is governed by an exogenous process. The entry of the vehicles into the ring road from the on-ramps is governed by ramp metering policies. The objective is to design ramp metering policies so as to keep the network undersaturated for a maximal combination of external demand and initial conditions. It is also of interest to analyze the impact of communication infrastructure between the vehicles and the ramp metering controllers, and coordination between the controllers on the ability to keep the traffic network undersaturated. We present a sample of our ongoing work in the form of two illustrative ramp metering policies and their performance analyses. A comprehensive treatment is being prepared for a journal paper submission, which also contains technical details which may have been omitted from this report for brevity.

4 Task 1: Modeling and analysis of traffic in a bounded space for different demand levels

Consider n homogeneous vehicles of length L, on a closed ring road. Without loss of generality, assume that the perimeter of the ring road is P for some $P > nL$. We assign coordinates over the distance interval $[0, P]$ to the ring road in the clock-wise direction. Let $\mathcal{N} = \{1, 2, \cdots, n\}$ be the set of vehicles' indices, where vehicle i is the i^{th}-closest vehicle to point 0 at time $t = 0$. Let $0 \leq x_i(t) < \infty$ denote the distance traveled by the i^{th} vehicle with respect to a fixed reference point on the roadside (without loss of generality we assume that this reference point is the point

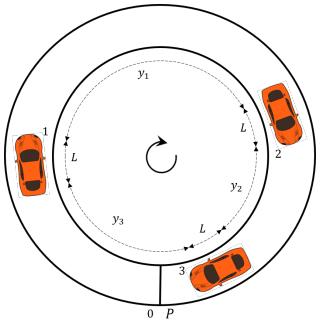

Figure 1: Example of three vehicles on a closed ring road setup

0), and $v_i(t)$, $a_i(t)$ denote the speed and acceleration at time $t \geq 0$, respectively. Moreover, let $y_i(t) = x_{i+1}(t) - x_i(t) - L$ be the relative spacing of the i^{th} vehicle with respect to the vehicle $i+1$ ahead at time $t \geq 0$, where $x_{n+1} \equiv P + x_1$ due to the periodicity of the ring road. Throughout the report, except when needed, we use x_i, v_i, a_i, and y_i without explicitly mentioning their dependence on time. For simplicity of notations, we formulate the vehicle model and controller design for an ego vehicle with subscript e and use the subscript l in order to differentiate between the ego vehicle and its immediate vehicle ahead, i.e., the lead vehicle. We must emphasize that the lead vehicle should not be confused with the leader of a platoon.

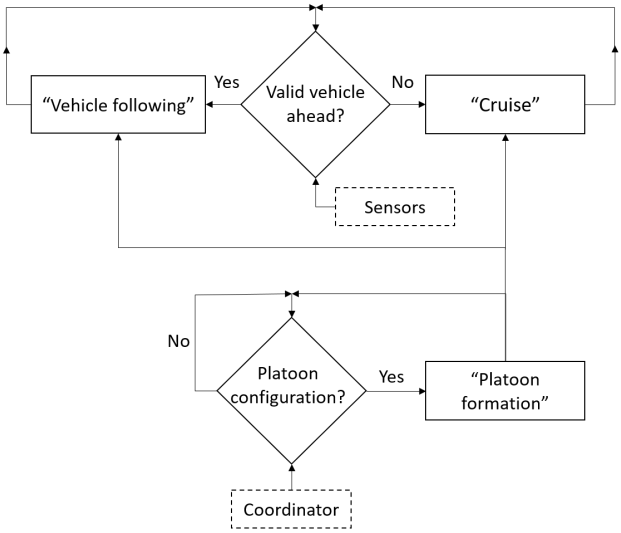

Figure 2: Logic diagram for determining the mode of operation

Note that by definition, $\sum_{i=1}^{n} y_i = P - nL$. This constraint is the main contrast to a straight line with no space limitation. An illustration of this setup for three vehicles is depicted in Figure 1.

4.1 Modes of Operation

Each vehicle operates in one of the following two modes of operation: cruise control or vehicle following, see Figure 2. If there is no coordination, an ego vehicle operates in the cruise mode if no valid vehicle is ahead that is within its sensing range. The validity of the lead vehicle is determined by comparing the relative spacing to a design threshold value. The ego vehicle is in the vehicle

following mode, i.e., it follows the lead vehicle by keeping a safety distance, as long as the lead vehicle's speed is within the allowable speed limit. The speed limit is taken to be equal to the free flow speed V_f when there is no coordination. The platoon formation state in Figure 2 is activated in order to achieve a desired platoon formation when a coordinator is present.

4.2 Vehicle Model

We assume that the road surface is horizontal and there is no wind gust. We use Newton's second law of motion for the ego vehicle to write,

$$m_e a_e = F_e - k_d v_e^2 - d_m(v_e)$$

where F_e is the engine force, m_e is the mass, k_d is the aerodynamic drag coefficient, and $d_m(v_e)$ is the mechanical friction of the ego vehicle travelling with the speed v_e [26]. Assuming a first-order engine dynamics we have,

$$\dot{F}_e = \frac{1}{\tau(v_e)}(\theta_e - F_e)$$

where θ_e is the throttle angle's force to the engine, and $\tau(v_e)$ is the engine's time constant at the speed v_i [27].

By combining the last two equations we derive,

$$\dot{a}_e = \beta(v_e, a_e) + \alpha(v_e)\theta_e$$

where,

$$\begin{aligned} \alpha(v_e) = & \frac{1}{m_e \tau(v_e)} \\ \beta(v_e, a_e) = & -2\frac{k_d}{m_e} v_e a_e - \frac{1}{m_e}\dot{d}_m(v_e) \\ & - \frac{1}{\tau(v_e)}[a_e + \frac{k_d}{m_e} v_e^2 + \frac{d_m(v_e)}{m_e}] \end{aligned}$$

At each speed v_e, throttle angle is chosen such that,

$$\theta_e = \frac{1}{\alpha(v_e)}[u_e - \beta(v_e, a_e)]$$

which leads to the equation,

$$\dot{a}_e = u_e \tag{1}$$

where u_e is to be designed to meet the control objectives presented below:

1. **Safety**: no rear-end collision under a worst-case stopping scenario as explained in [6]
2. **Smooth longitudinal maneuver**: Smooth position and/or speed tracking in the two modes of operation as well as a smooth transition between these modes
3. **String error attenuation**: attenuation of the amplitude of errors, e.g., in the position, upstream a platoon
4. **Passenger comfort**: $a_{min} \leq a_e \leq a_{max}$, except in an emergency braking scenario, and small jerk $\dot{a}_e$ [5]

In the following sections, we design and analyze control laws that can meet the objectives with and without V2V communication and in the presence of a coordinator.

4.3 No V2V Communication

In this section, we assume that vehicles do not communicate with each other and obtain the necessary data for cruising or vehicle following by using their own sensing capabilities. When the mode of operation is determined as explained in Section 4.1, the sensing data are passed through appropriate filters [16] in order to generate continuous-time signals passed to the longitudinal controller u_e designed as follows. It should be noted that controllers of similar form have been well-studied in the literature, e.g., see [16].

1. **Cruise**:

$$\begin{aligned} u_e = \; & K_a a_e + C_v(v_r - v_e) \\ & + \int_0^t [C_s(v_r - v_e)]d\tau \end{aligned} \tag{2}$$

$$\dot{v}_r = \; \text{sat}[p(V_s - v_r)], \; v_r(0) = v_e(0) \tag{3}$$

$$\text{sat}[x] = \begin{cases} a_{max} & \text{if} \;\; x \geq a_{max} \\ x & \text{if} \;\; a_{min} < x < a_{max} \\ a_{min} & \text{if} \;\; x \leq a_{min} \end{cases} \tag{4}$$

2. **Vehicle following**:

$$\begin{aligned} u_e = \; & K_a a_e + C_p(t)\delta_e + C_v(v_r - v_e) \\ & + \int_0^t [C_q(\tau)\delta_e + C_s(v_r - v_e)]d\tau \end{aligned} \tag{5}$$

$$v_r = \; v_l + (v_r(0) - v_l)e^{-\lambda t} \tag{6}$$

$$\delta_e = \; y_e - (hv_e + S_0) \tag{7}$$

where $K_a < 0$, $C_v, C_s, p, \lambda > 0$ are design constants, V_s is the speed limit and $V_s = V_f$. Moreover, the threshold distance Δ_d for switching from the cruise control mode to the vehicle following mode is chosen as follows,

$$\Delta_d = \begin{cases} hv_e + S_0 + r(v_e - v_l) & \text{if} \;\; v_e \geq v_l \\ hv_e + S_0 & \text{otherwise} \end{cases} \tag{8}$$

where $r > 0$ is a design constant. If the relative spacing of the ego vehicle with respect to the lead vehicle ahead is greater than Δ_d at $t = 0$, the ego vehicle starts operating in the cruise control mode and the speed tracking controller (2) is used. The reference speed v_r in this case is generated by passing the desired speed limit V_s through the nonlinear acceleration limiter filter (3) with the saturation function described in (4). The acceleration limiter prevents the acceleration outside the comfortable range when there is a large initial speed error $V_s - v_e(0)$ [5]. If the relative spacing becomes less than Δ_d at some time $t_0 \geq 0$, the ego vehicle switches to the vehicle following mode and the speed/position tracking controller (5) is used. The design parameters $C_p(t), C_q(t)$ are smoothly increased from zero to some positive design constants $C_p, C_q > 0$, i.e., $C_p(t) = C_p(1 - e^{-\lambda(t-t_0)})$, $C_q(t) = C_q(1 - e^{-\lambda(t-t_0)})$, $t \geq t_0$. Moreover, the reference speed v_r is smoothly changed from the

initial value to the speed of the lead vehicle v_l (see (6)), and the reference relative spacing is set to $hv_e + S_0$ (see (7)), where $S_0 > 0$ is a constant standstill separation distance and h is a safe time headway constant. This is a well-known safe vehicle following strategy where the following vehicles try to keep a safe constant time headway from the vehicle ahead [6]. It was shown that the value of the time headway constant can be chosen such that two consecutive vehicles do not collide under a worst-case stopping scenario as explained in [6]. Accordingly, the switching distance Δ_d is chosen to be equal to the safety distance $hv_e + S_0$ plus an additional non-negative term $r(v_e - v_l)$ if the ego vehicle is travelling at least as fast as the lead vehicle (see (8)). The ego vehicle keeps operating in the vehicle following mode as long as the lead vehicle's speed is within its allowable speed limit V_s.

Remark 1.
- *The objective is to design the control parameters such that* (2) - (8) *ensures stability, string error attenuation, and, lastly, satisfies comfort. We should emphasise that the designed longitudinal controller is only responsible for smoothly adjusting the spacing and/or speed. Other operations such as emergency braking are assessed by a higher-level supervisory controller and operated by different control laws which are not addressed in this report. However, this problem is resolved in other papers, see for example [5], [16].*

- *The ring road setting is a simple abstraction for bounded space. It is implicitly assumed that the perimeter of the road is large enough so that the lateral dynamics of the vehicle is negligible.*

We define $n_c = \frac{P}{hV_f + S_0 + L}$ as the *critical number of vehicles* on the ring road (n_c can be non-integer). We also define *configuration* as the vector of relative spacings on the ring road.

Theorem 1. *There exist design parameters such that the following hold:*

1. *The controller* (2) - (8) *guarantees smooth vehicle following and/or speed tracking in all modes of operation and string error attenuation, i.e., the attenuation of the amplitude of errors with respect to the desired relative spacing, speed, and acceleration upstream a platoon.*

2. *If $n < n_c$, there is an infinite number of vehicle configurations on the ring road; however the equilibrium speed is V_f in each of these configurations.*

3. *If $n \geq n_c$, there is a unique vehicle configuration where all vehicles are symmetrically distributed around the ring road and their speed converges to an equilibrium speed of $\frac{1}{h}(\frac{P}{n} - S_0 - L) \leq V_f$.*

Remark 2. *Simulations (and practical considerations) suggest that a vehicle in the vehicle following mode does not switch to cruise control under the proposed logic-based controller (see Figure 2). This implies that there is no switch in the overall mode of the system after finite time. Furthermore, within each mode, we show in the proof of Theorem 1 in [28] that the saturation constraints on the acceleration are not binding, and hence thereafter the system can be treated as an LTI system. In this sense, linear system tools are sufficient for asymptotic analysis.*

Remark 3. *The proof of Theorem 1 in [28] suggests that when in the cruise control mode, a vehicle satisfies the comfortable acceleration limits and when in the vehicle following mode, it accelerates/decelerates at most as high as the preceding vehicle except, maybe, for an exponentially vanishing term. We confirm via simulations that this guarantees the specified comfort requirements except, maybe, for an exponentially vanishing time.*

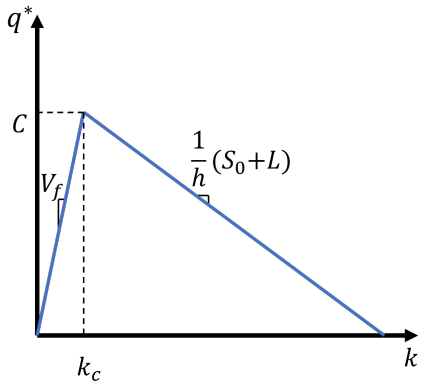

Figure 3: Fundamental diagram without V2V communication

Remark 4. *According to Theorem 1, for a given number of vehicles $n < n_c$, vehicles can form platoons of (possibly) different sizes with different inter-platoon spacing at steady state, which depends on the initial condition. We discuss in [28] the role of coordination in achieving a unique desired configuration in order to improve efficiency in utilizing the limited space.*

Remark 5. *Macroscopic traffic flow interpretation of Theorem 1: Let v^* be the equilibrium speed of vehicles, $k = \frac{n}{P}$ be the space-mean* density, *$k_c = \frac{n_c}{P}$ be the* critical density, *and $q^* = kv^*$ be the equilibrium space-mean* flow. *It follows from Theorem 1 that $v^* = \min\{V_f, \frac{1}{h}(\frac{P}{n} - S_0 - L)\}$. Therefore,*

$$q^* = \begin{cases} V_f k & \text{if } \ k < k_c \\ \frac{1}{h}(1 - k(S_0 + L)) & \text{if } \ k \geq k_c \end{cases}$$

In other words, when the density is less than the critical density, the flow increases linearly with increasing density. However, when the density exceeds the critical density, the flow decreases linearly with increasing density. This gives rise to the well-known triangular fundamental diagram (see Figure 3). The maximum value of q^*, i.e., the capacity *C of the ring road, is then found to be $C = \frac{V_f}{hV_f + S_0 + L}$.*

Remark 6. *According to the proof of Theorem 1 in [28], for speed tracking in the cruise control mode the poles of the transfer function from the reference speed to the speed of the ego vehicle must lie in the open left half of the s-plane. This condition is satisfied if,*

$$K_a C_v + C_s < 0 \tag{9}$$

Moreover, for position/speed tracking and string error attenuation in the vehicle following mode, the design parameters must be chosen such that poles of the transfer function from the speed of the lead vehicle to the speed of the ego vehicle have negative real parts and $|G(j\omega)| \leq 1$, $\forall \omega \geq 0$. The former can be guaranteed by using pole placement. Additionally, $|G(j\omega)| \leq 1$, $\forall \omega \geq 0$ is satisfied if,

$$\begin{aligned} C_1 &\geq 0 \\ C_2 - C_v^2 &\geq 0 \end{aligned} \tag{10}$$

where,

$$\begin{aligned} C_1 &= K_a^2 - 2(hC_p + C_v) \\ C_2 &= (hC_p + C_v)^2 + 2C_q + 2K_a(C_p + hC_q + C_s) \end{aligned}$$

We provide a set of parameters in Section 4.5 that satisfies (9) *and* (10) *(refer to* (12)*) as well as the stability criterion for* $G(s)$.

4.4 V2V Communication

We now assume that vehicles are able to communicate their braking capabilities as well as their instantaneous acceleration and deceleration to their following vehicle. This feature allows for accurate reference tracking when vehicles are outside the sensing range and also smaller safe time headway constant between vehicles [29]. With V2V communication, the longitudinal control law in the vehicle following mode (5) is modified as follows,

$$\begin{aligned} u_e = \; & K_a a_e + C_p(t)\delta_e + C_v(v_r - v_e) + C_a(t)(a_l - a_e) \\ & + \int_0^t [C_q(\tau)\delta_e + C_s(v_r - v_e) + C_b(\tau)(a_l - a_e)]d\tau \end{aligned} \tag{11}$$

where $C_a(t), C_b(t) \geq 0$ are additional control parameters which behave similar to $C_p(t), C_q(t)$. Note that the only difference between (5) and (11) is the additional acceleration terms $C_a(t)(a_l - a_e)$ and $C_b(t)(a_l - a_e)$ in (11). Since by choosing $C_a(t) = C_b(t) = 0$, $\forall t \geq 0$, (11) becomes identical to the control law in (5) all of the results for stability, string error attenuation, and comfort holds when V2V communication is possible. In fact, V2V communication adds additional degrees of freedom in choosing the design constants in order to guarantee good tracking performance.

As mentioned earlier, V2V communication reduces the minimum safe time headway constant h. Thus, the critical number of vehicle n_c for which vehicles can operate at the free flow speed increases. As a result, the critical density $k_c = \frac{1}{hV_f + S_0 + L}$ and the capacity $C = \frac{V_f}{hV_f + S_o + L}$ in Remark 5 are increased. Therefore, V2V communication expands the free-flow region of the Fundamental diagram.

Furthermore, using V2V communication, vehicles can be organized in platoons and decide among themselves certain configurations. Moreover, it allows for accurate tracking of the position, speed, and acceleration of the preceding vehicle even when they are outside the sensing range. This feature expands the number of possible configurations that can be achieved in the presence of a coordinator, e.g., see [28].

4.5 Simulation Results

In this section, we illustrate the performance of the designed control laws by simulating a few scenarios. In all scenarios, the control parameters are chosen as follows,

$$\begin{aligned} & K_a = -9, \;\; C_p = 2, \;\; C_v = 6, \;\; C_q = 0.01, \;\; C_s = 0.03 \\ & h = 1.5 \; [s], \;\; S_0 = 4 \; [m], \;\; p = 10, \;\; a_{min} = -0.2g \\ & a_{max} = 0.1g, \;\; r = 1, \;\; \lambda = 0.5 \end{aligned} \tag{12}$$

These design constants are chosen to ensure that stability, string error attenuation, and comfort conditions are satisfied; see [28] for further details. Other parameters are chosen to be as follows,

$$P = 320 \; [m], \;\; L = 4.5 \; [m], \;\; V_f = 29 \; [\frac{m}{s}]$$

Therefore, the critical number of vehicles is $n_c = \frac{320}{1.5 \times 29 + 4 + 4.5} = 6.04$.

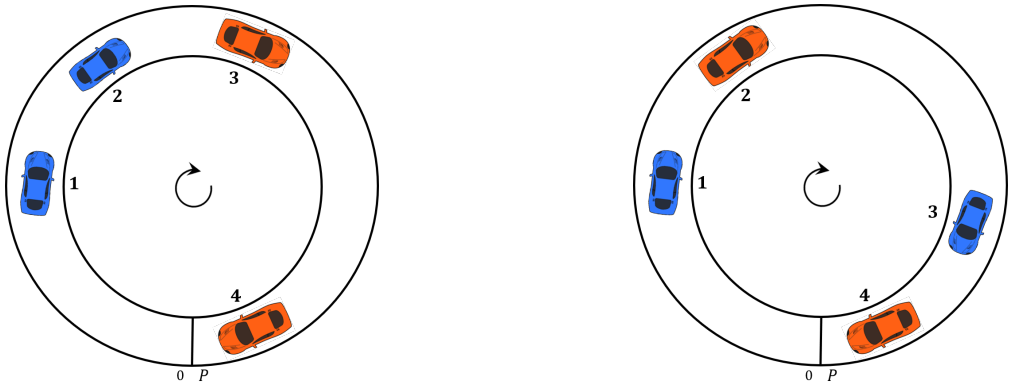

(a) (b)

Figure 4: Steady state configuration of vehicles when there is (a) no coordination, (b) coordination with 2-platoon symmetrical desired configuration, where vehicles in the cruise control mode are colored in orange and the ones in the vehicle following are colored blue

4.5.1 High Density Traffic Regime

Let $n = 8 > n_c$, i.e., a high-density traffic regime, with two platoons of sizes 3 and 5 initially at rest. The first platoon consists of vehicles $1-3$ with vehicle 3 as the leader, and the second platoon consists of vehicles $4-8$ with vehicle 8 as the leader. The distance between the first and second platoons is initially 100 meters, i.e., $y_3(0) = 100$ $[m]$, and all the following vehicles are assumed to be at the desired spacing at $t = 0$. According to Theorem 1, the system of vehicles converges to a unique configuration with the equilibrium relative spacing of $\frac{P}{n} - L = 35.5$ $[m]$, and speed of $\frac{1}{h}(\frac{P}{n} - S_0 - L) = 21$ $[\frac{m}{s}]$. The speed, acceleration, and relative spacing profiles for sample vehicles are shown in Figures 5. As can be seen from the acceleration and speed profiles, the leader of the first platoon, i.e., vehicle 3, operates in the cruise control mode until $t \approx 15$ $[s]$. At this point it switches to the vehicle following mode and the two platoons become connected. Furthermore, the leader of the second platoon switches to the vehicle following mode at $t \approx 26$ $[s]$, and a platoon with no leader [1] is formed. It is clear that the speed and acceleration profiles are smooth and within the comfort range in both modes of operation as well as during the transition between the two modes.

In connection to the fundamental diagram in Figure 3, it is seen that the density is $k \approx 40$ $[\frac{\text{veh}}{\text{mi}}]$ and the flow converges to $\frac{1}{h}(1 - k(S_0 + L)) \approx 1888$ $[\frac{\text{veh}}{\text{h}}]$ which is less than the capacity $C = \frac{V_f}{hV_f + S_0 + L} \approx 1995$ $[\frac{\text{veh}}{\text{h}}]$.

4.5.2 Low Density Traffic Regime: No Coordination

In this scenario, let $n = 4 < n_c$, i.e., a low-density traffic regime, and all vehicles are initially at rest. We assume that vehicles $1-3$ are initially in platoon formation with the following vehicles at the desired spacing, and vehicle 4 is 100 meters ahead. The speed, acceleration, and relative spacing profiles of the vehicles are shown in Figure 6. It can be seen from the relative spacing profiles that vehicles 3 and 4 operate in the cruise control mode at all times, thus at steady state, we have one platoon of three vehicles with vehicle 3 as the leader, and a single vehicle, i.e., vehicle 4, operating

[1] The term "platoon with no leader" in this report refers to the situation where all the vehicles are operating in the vehicle following mode.

in the cruise control mode, see Figure 4a. Moreover, it can be easily verified that all vehicles reach the free flow speed V_f while satisfying the the acceleration bounds during the transient. Also, it can be seen from the acceleration profiles that the errors in acceleration are not magnified upstream a platoon, i.e., string error attenuation.

4.5.3 Low Density Traffic Regime: With Coordination

We again consider $n = 4$. We assume that vehicles are travelling at steady state speed of V_f and initial configuration of the previous scenario. Let the coordinator's desired configuration be 2-platoon symmetrical with vehicles 2 and 4 as the desired leaders. The simulation results for this scenario are shown in Figure 7. The coordinator communicates the desired configuration to vehicles 2 and 4 at $t = 10$ $[s]$. Since the platoon consisting of vehicles 3 and 4 has not formed at $t = 10$ $[s]$, vehicle 4 sets its speed limit to $V_s = 0.8V_f$, and starts to decelerate until vehicle 3 catches up. At the same time vehicle 2 smoothly increases its time headway constant to the desired value $h_d \approx 3.43$ $[s]$, and starts decelerating in order to adjust its relative spacing. At $t \approx 20$ $[s]$, vehicle 3 switches to the vehicle following mode, and vehicle 4 resets its speed limit while smoothly increasing its desired relative spacing to $h_d v_1 + S_0$. Due to large initial positive relative spacing and speed error at $t \approx 20$ $[s]$, this introduces acceleration outside the comfortable bounds for vehicle 4. It can be seen from the relative spacing profiles at $t \approx 35$ $[s]$, that the desired configuration is achieved asymptotically. The qualitative steady state configuration of this scenario is shown in Figure 4b.

In contrast to the high-density case, the density in the last two cases are approximately 20 $[\frac{\text{veh}}{\text{mi}}]$, which is below the critical density $k_c \approx 30$ $[\frac{\text{veh}}{\text{mi}}]$. Therefore, the flow in both cases eventually converge to $V_f k = 1969$ $[\frac{\text{veh}}{\text{h}}]$. Note, however, that the transient flow profiles as well as the steady-state configuration is different in each case.

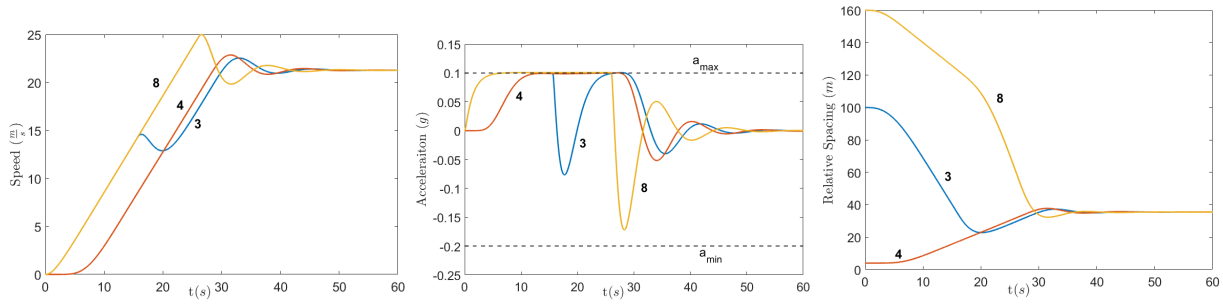

Figure 5: Simulation results for the high density traffic regime

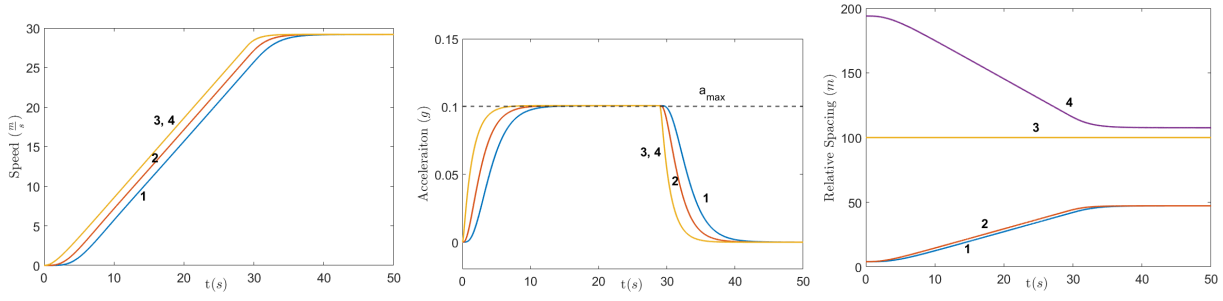

Figure 6: Simulation results for the low density traffic regime with no coordination

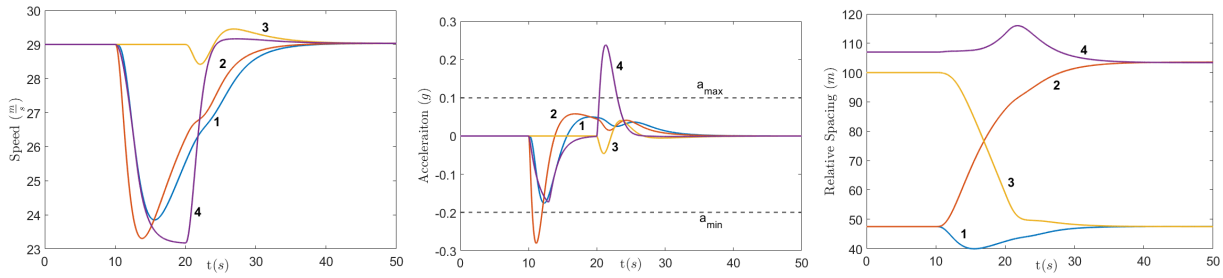

Figure 7: Simulation results with coordination and 2-platoon symmetrical desired configuration

5 Tasks 2 and 3: Modeling and analysis of traffic over network with entries and exits for different demand levels

We discuss results for Tasks 2 and 3 together since they both deal with entry and exit of vehicles.

5.1 Problem Setup

Let there be m on- and off- ramps, as illustrated in Figure 8. The on- and off-ramps are placed alternately, and they are numbered in an increasing order along the clockwise direction. The road segment between on-ramps j and $j+1$ is referred to as the *link* j.

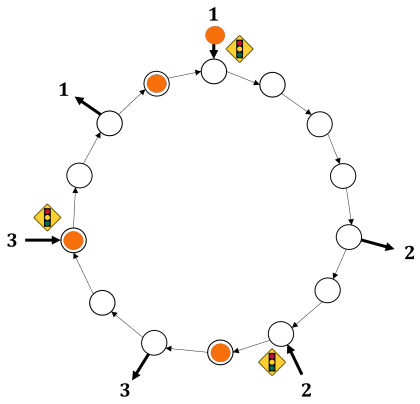

Figure 8: Idealized graph of the problem setup with $m = 3$ on/off-ramps and $n_c = 14$ virtual slots

5.1.1 Vehicle Level Controller

We adopt the control framework in similar spirit, but not restricted, to Section 4.3. Specifically, safety considerations can be naturally divided into two scenarios: (a) vehicle-following on the ring road, and (b) merging from on-ramp into the ring road.

Vehicle Following Let the speeds of the ego and the leading vehicles be denoted by v_e and v_l, respectively.

1. If v_e is approximately equal to v_l, then the ego vehicle tries to keep a constant time headway $h > 0$ plus an additional constant gap $S_0 > 0$ [6], i.e., the safety distance in this case is $hv_e + S_0$. This rule is widely adopted by human drivers as well as in standard adaptive cruise control systems.

2. If v_e is greater than v_l, then the ego vehicle starts to decelerate at a safe distance S_e that scales with the difference of square of speed, i.e., $S_e = hv_e + S_0 + \frac{v_e^2 - v_l^2}{2|a_{min}|}$, where $a_{min} < 0$ is the minimum possible deceleration of the lead vehicle. This distance accounts for an emergency braking scenario as explained in [6].

Merging We consider ramp metering policies which release vehicles into the ring road only if the distance of the merging vehicle from the upstream and downstream vehicles do not violate the safety distance required in an emergency braking situation.

It is natural to assume that the initial condition of vehicles on the ring road is such that it satisfies the safety constraints. In particular, this implies that the initial number of vehicles is no more than $P/(S_0 + L)$. Under the safe merging constraint on the ramp metering policies, this also ensures that the number of vehicles on the ring road are also upper bounded by $P/(S_0 + L)$ at all times.

We do not assume a specific vehicle controller. We do however require the controllers to be such that there exists $T_{\text{empty}} > 0$ such that, starting from any safe configuration, all the vehicles on the ring road reach their destination off-ramps in time T_{empty} if no additional vehicles enter the ring road during this time. This is satisfied, e.g., by the controllers considered in Section 4.3.

5.1.2 Demand Model

It is convenient for performance analysis to adopt a discrete time setting. Let the time step be $h + \frac{S_0+L}{V_f}$, representing the minimum safe time headway between two consecutive vehicles that are moving at the free flow speed. To conveniently track vehicle locations on the ring road in discrete time, we introduce the notion of *slots*. A slot is associated with a particular point on the ring road. Let n_c be the maximum number of distinct points that can be placed on the ring road, such that the distance between adjacent points is $hV_f + S_0 + L$. This distance is governed by safety considerations (see Section 5.1.1). Without loss of generality, consider such a configuration of slots at $t = 0$ so that each on-/off- ramp has a slot in front of it. The slots are numbered in an increasing order in the clockwise direction, with the slot in front of on-ramp 1 assigned number 1. Thereafter, during each time step, the following sequence of events occurs: (i) the slots rotate one position in the clockwise direction; without loss of generality, we let n_c and the location of on/off-ramps be such that, after rotation, each on- and off-ramp has a slot in front of it; the numbering of slots is reset with the new slot in front of on-ramp 1 numbered 1, and the rest numbered in an increasing order in the clockwise direction, (ii) vehicles that reach their destination off-ramp exit the network, (iii) every on-ramp releases a vehicle into a safe slot, if permitted by ramp metering.

The following abstraction is inspired by similar problems studied in the queueing literature, e.g., see [30]. Let vehicles arrive to on-ramp $i \in [m]$ according to an i.i.d. Bernoulli process with parameter $\lambda_i \in [0, 1]$. These processes are independent across the on-ramps. That is, in any given time step, the probability that a vehicle arrives at the i^{th} on-ramp is λ_i independent of everything else. We refer to the parameter λ_i as the *arrival rate* to on-ramp i and we let $\lambda := [\lambda_i]$ be the vector of arrival rates to the network. The destination off-ramp for individual arriving vehicles is i.i.d. and is given by a *routing matrix* $R = [R_{ij}]$, where $0 \leq R_{ij} \leq 1$ is the probability that an arrival

to on-ramp i wants to exit from off-ramp j. Naturally, for every on-ramp i we have $\sum_j R_{ij} = 1$. Finally, we let $\tilde{R} = [\tilde{R}_{ij}]$ be the *cumulative* routing matrix, where $\tilde{R}_{ij}$ is the fraction of arrivals at on-ramp i that needs to cross off-ramp j in order to reach their destination (this includes the vehicles that need to exit from off-ramp j). Note that $\sum_j \tilde{R}_{ij}$ indicates the fraction of arrivals at all on-ramps that needs to cross off-ramp j in order to reach their destination.

Example 1. *Let the routing matrix for a 3-ramp network (see, for example, Figure 8) be given by*

$$R = \begin{pmatrix} R_{11} & R_{12} & R_{13} \\ R_{21} & R_{22} & R_{23} \\ R_{31} & R_{32} & R_{33} \end{pmatrix}$$

Then, the cumulative routing matrix is calculated as follows:

$$\tilde{R} = \begin{pmatrix} 1-(R_{12}+R_{13}) & 1 & 1-R_{12} \\ 1-R_{23} & 1-(R_{23}+R_{21}) & 1 \\ 1 & 1-R_{31} & 1-(R_{31}+R_{32}) \end{pmatrix} = \begin{pmatrix} R_{11} & 1 & R_{11}+R_{13} \\ R_{21}+R_{22} & R_{22} & 1 \\ 1 & R_{32}+R_{33} & R_{33} \end{pmatrix}$$

Let $\rho_j := \sum_i \lambda_i \tilde{R}_{ij}$ be the average rate of arrivals that need to cross link $j-1$ in order to reach their destination off-ramp, and let $\rho := \max_{j\in[m]} \rho_j$ be the *average load* in the network.

5.1.3 Saturation Limit and Ramp Metering

The key performance metric here is the *saturation limit* of the network. For $i \in [m]$, let $Q_i(t)$ be the set of destination off-ramps of the vehicles waiting at on-ramp i, arranged in the order of their arrival, at t. We assume a point queue model for vehicles waiting at the on-ramp, with the queue co-located with the on-ramp. Therefore, $|Q_i(t)|$ denotes the queue length at on-ramp i at time t. Let $|Q(t)|$ be the vector of queue lengths at all the on-ramps at time t. Recall the placement of slots on the ring road and their numbering scheme. Let $M(t)$ be the set of the destinations of the occupants of the n_c slots on the ring road: $M_\ell(t) = j$ if the destination of the vehicle occupying slot ℓ at time t is off-ramp j, and $M_\ell(t) = 0$ if slot ℓ is empty at time t. $|M(t)|$ is therefore the number of vehicles on the ring road at time t.

We consider ramp metering policies of the form $\pi : |Q(t)| \times |M(t)| \to \{0,1\}^m$. On-ramp i releases a vehicle into the slot in front at time t only if it is safe and $\pi_i(t) = 1$. Note that ramp metering policies do not have access to the destination information of vehicles.

The network is said to be under-saturated under a given demand (λ, R) and ramp metering policy π if $\limsup_{t\to\infty} E[|Q_i(t)|] < \infty$ for all $i \in [m]$; otherwise, it is called saturated. We are interested in finding ramp metering policies which keep the network under-saturated for maximal combinations of (λ, R).

5.1.4 A Necessary Condition for Under-saturation

We first develop a necessary condition for under-saturation, against which we benchmark the sufficient condition for the ramp metering policies we design. To this purpose, let $\bar{D}_{\pi,p}(t)$ be the cumulative number of vehicles that has crossed point p on the ring road up to time t under a ramp-metering policy π. Then, the crossing rate at point p is defined as $\bar{D}_{\pi,p}(t)/t$ and the "long-run" crossing rate is $\limsup_{t\to\infty} \bar{D}_{\pi,p}(t)/t$.

Proposition 1. *Suppose that, for a given ramp metering policy, the long-run crossing rate is no more than one for at least one point on every link. If the network is under-saturated, then the demand must satisfy $\rho < 1$.*

5.2 A Decentralized Policy with No V2I Communication

Definition 1. ***(Fixed-Cycle Quota Ramp Metering (FCQ-RM) policy)*** *The policy works in cycles of fixed length $T \in \mathbb{N}$. At the beginning of the k^{th} cycle at $t_k = (k-1)T$, for all $k \geq 1$, each on-ramp allocates itself a "quota" equal to the queue length at that on-ramp at t_k. During the cycle $t \in [t_k, t_{k+1}]$, each on-ramp releases a vehicle whenever an empty slot appears, until it reaches its quota. Once an on-ramp reaches its quota, it does not release a vehicle during the rest of the cycle.*

Theorem 2. *Let the initial speed of all the vehicles on the ring road be V_f, and let the merging speed at all the on-ramps be V_f. For any cycle length T, the FCQ-RM policy keeps the network under-saturated if and only if $\rho < 1$.*

Note that, in spite of being decentralized, the FCQ-RM policy may not guarantee under-saturation for all initial conditions. As we show next, this can be addressed through V2I communication from all vehicles on the ring road to each on-ramp. Whether this can be achieved by a more local communication protocol is under investigation.

5.3 A Centralized Policy with V2I Communication

The key idea here is to impose minimum time gap between release of successive vehicles from on-ramps on top of FCQ-RM, where this minimum time gap is dynamically updated based on traffic condition.

Definition 2. ***(Adaptive FCQ-RM (aFCQ-RM) policy)*** *The policy works in cycles of fixed length $T \in \mathbb{N}$. At the beginning of the k^{th} cycle at $t_k = (k-1)T$, for all $k \geq 1$, each on-ramp allocates itself a "quota" equal to the queue length at that on-ramp at t_k. During the cycle $t \in [t_k, t_{k+1}]$, the j^{th} on-ramp releases a vehicle if a safe virtual slot appears, and at least $g(t)$ time has passed since the release of the last vehicle. Once an on-ramp reaches its quota, it does not release a vehicle during the rest of the cycle.*

The minimum time gap $g(t)$ is piecewise constant, updated periodically at $t = T_{per}, 2T_{per}, \ldots$, as described in Algorithm 1. The state of vehicle e is $x_e^T = (v_e - V_f, a_e)$ in the cruise control mode, where a_e is its acceleration, and is $x_e^T = (y_e - (hv_e + S_0), v_e - V_f, a_e)$ in the vehicle following mode, where y_e is the distance to the leading vehicle. The state of all the vehicles is collectively denoted as $X^T = (\{x_e^T\}_{e \in [n]})$

Algorithm 1 Update rule for the minimum time gap between release of vehicles under the aFCQ-RM policy

Require: $T_{\text{per}} > 0, \alpha > 0, \theta > 0, g(0) = 0$
for $t = T_{\text{per}}, 2T_{\text{per}}, \cdots$ **do**
  if $\|X(t)\| = 0$ **then**
    $g(t) \leftarrow 0$
  else
    if $\|X(t)\| < \|X(t - T_{\text{per}})\| - \alpha$ **then**
      $g(t) \leftarrow g(t - T_{\text{per}})$
    else
      $g(t) \leftarrow g(t - T_{\text{per}}) + \theta$
    end if
  end if
end for

Proposition 2. *Let the merging speed at all the on-ramps be V_f. For any cycle length T and positive design constants T_{per}, α, θ, the aFCQ-RM policy keeps the network under-saturated if and only if $\rho < 1$.*

5.4 Performance Analysis Approach

The detailed proofs of Theorem 2 and Proposition 2 will be presented in a forthcoming journal paper. A key technical step is to cast the traffic network under a ramp metering control as a discrete-time Markov chain with state

$$Y_{\triangle}(t) := (X_{\mathrm{MC}}(t),\ X_{\mathrm{MC}}(t-1),\ \cdots,\ X_{\mathrm{MC}}(t-\triangle+1)),\ t \geq \triangle - 1$$

where $X_{\mathrm{MC}}(t) := (Q(t), \pi(t))$, and $\triangle \in \mathbb{N}$ will be specified for the policy being analyzed. The transition probabilities are also determined by the ramp metering policy. The function

$$V_{\triangle}(t) \equiv V\left(Y_{\triangle}(t)\right) := \sum_{s=t-\triangle+1}^{t} N^2(s) \tag{13}$$

plays an important role in the analysis. Note that (13) implies $V_{\triangle}(t+1) - V_{\triangle}(t) = N^2(t+1) - N^2(t-\triangle+1)$. The following is an adaptation of a well-known result, e.g., see [31, Theorem 14.0.1], for the setting of our paper.

Theorem 3. ***(Foster-Lyapunov drift criterion)*** *Let $\{Z(t)\}_{t=1}^{\infty}$ be an irreducible and aperiodic discrete time Markov chain evolving on a countable state space $\mathcal{Z}$. Suppose that there exist $V : \mathcal{Z} \to [0, \infty)$, $f : \mathcal{Z} \to [1, \infty)$, a finite constant b, and a finite set $B \in \mathcal{Z}$ such that, for all $z \in \mathcal{Z}$,*

$$\mathbb{E}V\left(Z(t+1)\right) - V\left(Z(t)\right) \,|\, Z(t) = z \leq -f(z) + b\mathbb{1}_B(z), \tag{14}$$

where $\mathbb{1}_B(z)$ is the indicator function of the set B. Then, $\lim_{t\to\infty} \mathbb{E}f(Z(t))$ exists and is finite.

5.5 Simulation Results

In this section, we provide simulation for the FCQ-RM policy. We use a ring road of length $P = 620$ $[m]$ with two on/off-ramps and $V_f = 15$ $[m/s]$. The on-ramps (resp. off-ramps) are located at the $[0 \quad P/2]$ (resp. $[P - 3(hV_f + S_0 + L) \quad P/2 - 3(hV_f + S_0 + L)]$) coordinates, and they are assumed to be empty at $t = 0$. Vehicles arrive according to i.i.d Bernoulli processes with the same rate λ, and are routed by

$$R = \begin{pmatrix} 0.8 & 0.2 \\ 0.5 & 0.5 \end{pmatrix}.$$

Note that, on average, most of the vehicles exit from off-ramp 1. Thus, under a greedy policy, one should expect that on-ramp 1 finds more empty virtual slots than on-ramp 2. Equivalently, the on-ramp 2's queue should be longer than on-ramp 1's. We assume that vehicles are homogeneous and autonomous, i.e., each vehicle uses the control law (2)-(8) with design constants in 4.5 (thus, platoons of vehicles are stable and string stable). For this choice of design constants, $n_c = 20$.

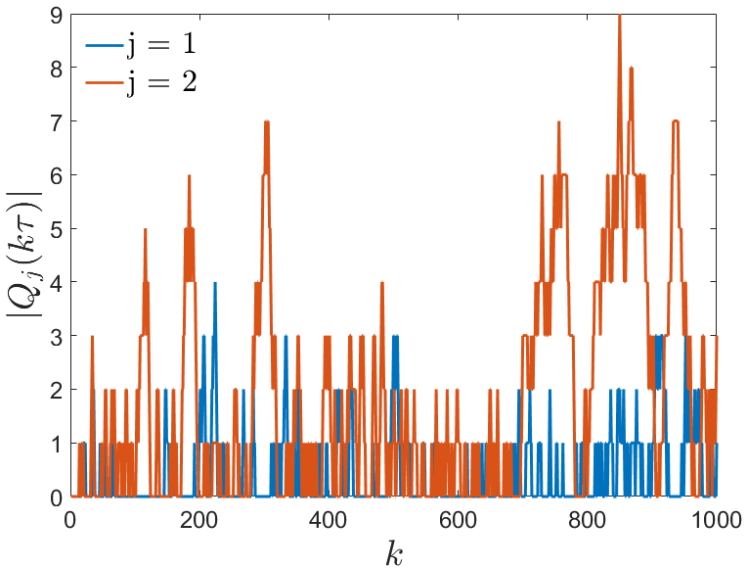

Figure 9: Queue length profiles in heavy traffic (merge speed at both on-ramps is the speed limit V_f).

5.5.1 The Greedy Policy

In this scenario, we simulate the performance of the greedy policy, i.e., the FCQ-RM with $T = 1$, for "heavy" traffic. We assume that the ring road is initially empty.

We assume that the merging speeds of both on-ramps is V_f. Thus, the network's saturation limit is $\{\lambda < 5/9\}$. The queue length profiles of both ramps for $\lambda = 0.5$ (so that $\rho = 0.9$) are shown in Figure 9 for $N = 1000$ time steps. As can be seen, the queue at on-ramp 2 is generally longer than that at on-ramp 1 due to the choice of routing matrix and the use of a greedy policy.

5.5.2 Comparing The Average Queue Lengths

In this section, we compare the long-run average queue lengths induced by the FCQ-RM policies with $T = 1, 5, 10, 50$ under different loads. We use the *batch means* approach in order to estimate the average queue lengths. We choose the warm-up period of the batch means method to be 10^5, i.e., the first 10^5 observations are not used, and use batches of size 10^5. In each case, the simulations are run until the margin of error of the 95% confidence intervals are 1%. We assume that the ring road is initially empty.

Figure 10 shows the simulation results when the merge speed at both on-ramps is the speed limit V_f. As can be seen, the greedy policy induces the lowest average queue lengths for all values of ρ. Figure 10 also shows that the greedy policy has very low average queue length even when ρ is near 1.

6 Conclusion

We considered the design of vehicle longitudinal controllers for homogeneous vehicles following a single lane in a closed ring road under safety and comfort constraints in order to evaluate the impact of limited space on the speed of flow. We showed that if the number of vehicles is less than a certain critical number n_c, which depends on the perimeter of the ring road, free flow speed

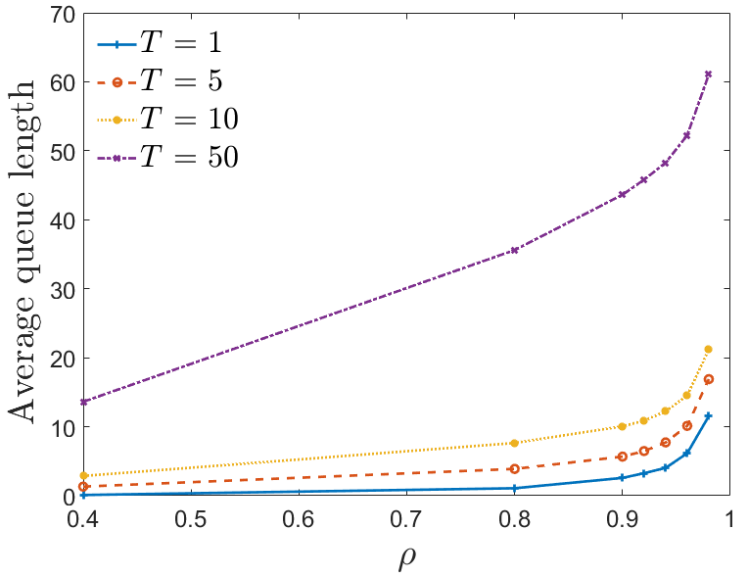

Figure 10: Average queue lengths (merge speed at both on-ramps is the speed limit V_f).

limit, and safety spacing, the vehicles can organize themselves around the ring road in an infinite number of different configurations. When the number of vehicles increases to be greater than or equal to n_c, all vehicles converge to a unique equilibrium configuration where the equilibrium speed decreases as the number of vehicles increases. When we add vehicle to vehicle communications, the controller is modified for faster action during vehicle following and safety can be guaranteed under lower inter-vehicle spacing. As a result, the critical number of vehicles n_c that can operate at the maximum allowable speed increases.

We then extended the setup to allow entry and exit of vehicles, with entry modulated by microscopic ramp metering. Inspired by spatial queues from communication network literature, we formulate a notion of saturation limit for the transportation network, and propose ramp metering policies which achieve the maximum possible saturation limit. Future work will aim at adding more breadth to performance analysis in terms of relaxing modeling assumptions, considering finite queue storage capacity at the on-ramps, travel time analysis for undersaturated conditions, as well as considering different communication and coordination architectures among the vehicles and ramp meters.

7 Implementation

Not applicable.

8 References

References

[1] David Schrank, Bill Eisele, Tim Lomax, and Jim Bak. 2015 urban mobility scorecard. 2015.

[2] Faisal Alasiri, Yihang Zhang, and Petros A. Ioannou. Robust variable speed limit control with respect to uncertainties. *European Journal of Control*, 2020.

[3] Pravin Varaiya. Smart cars on smart roads: problems of control. *IEEE Transactions on automatic control*, 38(2):195–207, 1993.

[4] J. Rios-Torres and A. A. Malikopoulos. A survey on the coordination of connected and automated vehicles at intersections and merging at highway on-ramps. *IEEE Transactions on Intelligent Transportation Systems*, 18(5):1066–1077, May 2017.

[5] P. Ioannou and Z. Xu. Throttle and brake control systems for automatic vehicle following. *I V H S Journal*, 1(4):345–377, 1994.

[6] P.A. Ioannou and C.C Chien. Autonomous intelligent cruise control. *IEEE Transactions On Vehicular Technology*, 42(4):657–672, 1993.

[7] Hedrick J.K. Swaroop D.D. Constant spacing strategies for platooning in automated highway systems. *ASME. J. Dyn. Sys., Meas., Control*, 121(3):462–470, 1999.

[8] E. Shaw and J. K. Hedrick. String stability analysis for heterogeneous vehicle strings. In *2007 American Control Conference*, pages 3118–3125, July 2007.

[9] H.S. Tan, R. Rajamani, and W.B. Zhang. Demonstration of an automated highway platoon system. In *Proceedings of the 1998 American Control Conference. ACC (IEEE Cat. No.98CH36207)*, volume 3, pages 1823–1827 vol.3, June 1998.

[10] P. Seiler, A. Pant, and K. Hedrick. Disturbance propagation in vehicle strings. *IEEE Transactions on Automatic Control*, 49(10):1835–1842, Oct 2004.

[11] P. Barooah, P. G. Mehta, and J. P. Hespanha. Mistuning-based control design to improve closed-loop stability margin of vehicular platoons. *IEEE Transactions on Automatic Control*, 54(9):2100–2113, Sep. 2009.

[12] Y. Zhang, B. Kosmatopoulos, P. A. Ioannou, and C. C. Chien. Using front and back information for tight vehicle following maneuvers. *IEEE Transactions on Vehicular Technology*, 48(1):319–328, Jan 1999.

[13] F. Lin, M. Fardad, and M. R. Jovanovic. Optimal control of vehicular formations with nearest neighbor interactions. *IEEE Transactions on Automatic Control*, 57(9):2203–2218, Sep. 2012.

[14] Kai-ching Chu. Decentralized control of high-speed vehicular strings. *Transportation Science*, 8(4):361–384, 1974.

[15] Peter Joseph Seiler. *Coordinated control of unmanned aerial vehicles*. University of California, Berkeley, 2001.

[16] H Raza and P Ioannou. Vehicle following control design for automated highway systems. *IEEE Control Systems Magazine*, 16(6):43–60, 1996.

[17] DVAHG Swaroop. *String stability of interconnected systems: An application to platooning in automated highway systems*. PhD thesis, University of California, Berkeley, 1994.

[18] S. Cui, B. Seibold, R. Stern, and D. B. Work. Stabilizing traffic flow via a single autonomous vehicle: Possibilities and limitations. In *2017 IEEE Intelligent Vehicles Symposium (IV)*, pages 1336–1341, June 2017.

[19] Yang Zheng, Jiawei Wang, and Keqiang Li. Smoothing traffic flow via control of autonomous vehicles. *IEEE Internet of Things Journal*, 7(5):3882–3896, 2020.

[20] Jiawei Wang, Yang Zheng, Qing Xu, Jianqiang Wang, and Keqiang Li. Controllability analysis and optimal control of mixed traffic flow with human-driven and autonomous vehicles. *IEEE Transactions on Intelligent Transportation Systems*, 2020.

[21] Yuki Sugiyama, Minoru Fukui, Macoto Kikuchi, Katsuya Hasebe, Akihiro Nakayama, Katsuhiro Nishinari, Shin-ichi Tadaki, and Satoshi Yukawa. Traffic jams without bottlenecks—experimental evidence for the physical mechanism of the formation of a jam. *New journal of physics*, 10(3):033001, 2008.

[22] Raphael E Stern, Shumo Cui, Maria Laura Delle Monache, Rahul Bhadani, Matt Bunting, Miles Churchill, Nathaniel Hamilton, Hannah Pohlmann, Fangyu Wu, Benedetto Piccoli, et al. Dissipation of stop-and-go waves via control of autonomous vehicles: Field experiments. *Transportation Research Part C: Emerging Technologies*, 89:205–221, 2018.

[23] Vittorio Giammarino, Simone Baldi, Paolo Frasca, and Maria Laura Delle Monache. Traffic flow on a ring with a single autonomous vehicle: An interconnected stability perspective. *IEEE Transactions on Intelligent Transportation Systems*, 2020.

[24] Sergei S Avedisov, Gaurav Bansal, and Gábor Orosz. Impacts of connected automated vehicles on freeway traffic patterns at different penetration levels. *IEEE Transactions on Intelligent Transportation Systems*, 2020.

[25] Milad Pooladsanj, Ketan Savla, and Petros Ioannou. Vehicle following over a closed ring road under safety constraint. In *2020 IEEE Intelligent Vehicles Symposium (IV)*, pages 413–418. IEEE.

[26] Reggie J. Caudill and William L. Garrard. Vehicle-follower, longitudinal control for automated transit vehicles. *IFAC Proceedings Volumes*, 9(4):195 – 209, 1976. IFAC/IFIP/IFORS 3rd International Symposium on Control in Transportation Systems, Columbus, Ohio, 9-13 August.

[27] Shahab E. Sheikholeslam. *Control of a Class of Interconnected Nonlinear Dynamical Systems: The Platoon Problem*. PhD thesis, EECS Department, University of California, Berkeley, 1991.

[28] M. Pooladsanj, K. Savla, and P. Ioannou. Vehicle following on a ring road under safety constraints: Role of connectivity and coordination. *IEEE Transactions on Intelligent Vehicles*, 2022.

[29] Vicente Milanés, Steven E Shladover, John Spring, Christopher Nowakowski, Hiroshi Kawazoe, and Masahide Nakamura. Cooperative adaptive cruise control in real traffic situations. *IEEE Transactions on intelligent transportation systems*, 15(1):296–305, 2013.

[30] Leonidas Georgiadis, Wojciech Szpankowski, and Leandros Tassiulas. A scheduling policy with maximal stability region for ring networks with spatial reuse. *Queueing Systems*, 19(1):131–148, 1995.

[31] Sean P Meyn and Richard L Tweedie. *Markov chains and stochastic stability*. Springer Science & Business Media, 2012.

9 Data Management Plan

Products of Research

No new data was collected for this project. Only simulation data was generated.

Data Format and Consent

All the simulations were done in Matlab.

Data Access and Sharing

The input/output data for the simulations in this report is available at `https://viterbi-web.usc.edu/~ksavla/code.html`.

Reuse and Redistribution

The data can be reused freely for non-commercial purposes. Its usage, in original or after modification, in publications is to be done with due acknowledgement to the authors of this report and by citation of relevant publications by the authors.